International Journal of Computational and Experimental Science and ENgineering (IJCESEN)

Vol. 12-No.1 (2026) pp. 362-370

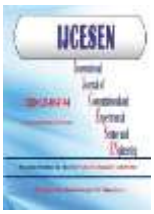

ISSN: 2149-9144

Research Article

Optimal Energy Management of a Microgrid Using Walrus Optimizer Algorithm

Mallem Aicha[1*], Benzaid Lamia[2], Lekhchine Salima[3], Bouloukza Ibtissam[4]

[1]Department of Electrical Engineering, LES Laboatory, University of 20 August 1955 -Skikda, Algeria
*** Corresponding Author Email**:a.mallem@univ-skikda.dz - **ORCID:** 0009-0001-5826-2359

[2]Department of Mechanical Engineering, Faculty of Technology,, University of 20 August 1955 -Skikda, Algeria
Email:l.benzaid@univ-skikda.dz - **ORCID:** 0009-0000-2933-6120

[3]Department of Electrical Engineering, LGMM Laboratory, University of 20 August 1955-Skikda, Algeria
Email: s.lekhchine@univ-skikda.dz - **ORCID:** 0000-0002-4509-5838

[4]Department of Electrical Engineering, Faculty of Technology, University of 20 August 1955 -Skikda, Algeria
Email: i.bouloukza@univ-skikda.dz - **ORCID:** 0000-0001-6976-973X

Article Info:

DOI: 10.22399/ijcesen.4785
Received: 08 October 2025
Revised: 09 December 2025
Accepted: 24 December 2025

Keywords

Energy management
Microgrid
Renewable energy
Distributed generator
Walrus Optimizer algorithm

Abstract:

The economic operation of electrical systems is very crucial. Efficient energy management can lower operating costs, improve grid stability, and optimize resource allocation. This paper proposes a novel technique based on the walrus optimizer (WaO) algorithm for solving the optimal energy management (OEM) of a microgrid (MG) based on the IEEE 33-bus system topology. The investigated system incorporates several distributed energy resources (DERs), such as photovoltaic (PV) and wind turbine (WT) units, micro-turbine (MT), diesel generator (DG), and battery energy storage system (BESS). To assess the robustness of the proposed strategy, three separate pricing situations are simulated: stable, moderate volatility, and high volatility. The results show the algorithm's capacity to perform optimal energy arbitrage and peak shaving, ensuring power balance and lowering grid reliance during high-price periods.

1. Introduction

The increased use of renewable energy sources (RESs) in distribution networks has hastened the development of microgrids (MGs). Modern MGs are self-managed electrical systems that can operate in either grid-connected or islanded modes, incorporating distributed energy resources (DERs) such as renewable generators, traditional fossil-fuel units, and energy storage devices. An energy management system (EMS) is necessary for efficient DER scheduling to ensure economic efficiency, environmental sustainability, and reliable operation [1], [2].However, the intermittent nature of RES and the unpredictability of energy market prices provide substantial obstacles for EMS. Traditional optimization methods, such as linear programming and dynamic programming, frequently fail to identify the global optimum in such complicated, multi-modal search spaces [3]. To solve these difficulties, the MG idea has emerged as a feasible option, enabling localized coordination of DEGs, storage systems, and loads.The optimal energy management (OEM) is a nonlinear optimization problem with constraints. The fundamental goal of an OEM within a MG is to establish each source's optimal output in order to reduce global operational costs while meeting technical limits. This problem has traditionally been addressed using classical optimization methods; however, the non-linear and non-convex character of modern MGs lends itself to the application of bio-inspired metaheuristic algorithms [4], [5].Several metaheuristic methods have been utilized to address OEM, such as: genetic algorithms (GA) [6], gravitational search algorithm (GSA) [7], differential evolution (DE) [8], cuckoo search [9], Particle swarm optimization (PSO) [10], Backtracking search optimization (BTA) [11], bacterial foraging [12], artificial bee colony (ABC) [13], grey wolf optimization [14], Moth-swarm algorithm [15]…etc. In this work, the walrus optimizer (WaO) approach is used to solve the OEM problem. The study is applied on a modified IEEE 33-bus test system over a 24-hour period. The key contribution of this paper is a comparison examination of the system's performance under three

realistic pricing scenarios, which shows the economic benefits of intelligent storage management and demand response.

2. Problem formulation

The OEM problem is an optimization problem. Its main objective is to minimize the operational costs of the MG, although further objectives may be added. The OEM problem can typically be articulated as:

$$C = \sum_{T=1}^{N^T} \left[C_{DEG_i}^T\left(P_{DEG_i}^T\right).\varphi_{i_i}^T + C_{\text{BESS}}^T + C_{\text{Gr}}^T \cdot P_{\text{Gr}}^T\right] \quad (1)$$

Where C represents the cost function over the entire planning horizon. P_{Gr}^T is the active power that is exchanged with the grid at time T. N^T represents the overall tally of time. $P_{DEG_i}^T$, $C_{DEG_i}^T$, C_{BESS}^T, and C_{Gr}^T refer to the active power output of the i[th] DEG, cost function of the i[th] DEG, cost function of the battery, and the electricity exchange price between of the grid at time T [16]. $\varphi_{i_i}^T$ is either 1 or 0, depending on whether the ith power supply is operational or not.

2.1. Micro-turbine (MT)

The MT cost function is presented as:

$$C_{\text{MT}} = a_{MT}P_{MT}^2 + b_{MT}P_{\text{MT}} + c_{MT} \quad (2)$$

Where a_{MT}, b_{MT}, and c_{MT} are the coefficients of MT cost function. P_{MT} represents MT output power.

2.2. Diesel generators (DG)

The cost function of the DG can be represented as:

$$C_{DG} = a_d P_{DG}^2 + b_d P_{DG} + c_{DG} \quad (3)$$

Where a_d, b_d, and c_d are the coefficients of DG cost function. P_{DG} represents DG output power.

2.3. Battery storage

The cost of the battery is an operational cost based on the power exchanged. It can be defined as:

$$C_{BESS} = b_{BESS}.P_{BESS} \quad (4)$$

2.4. PV and wind turbine (WT)

The output power of the solar PV system is influenced by solar irradiation, the site's ambient temperature, and the module's characteristics. The PV output power can be calculated using the following equation [17]:

$$P_{PV}(t) = N.\delta_{PV}.A_{PV}.S(t) \quad (5)$$

Where P_{PV}, δ_{PV}, A_{PV}, N and S represent the output power of the PV arrays, efficiency of power generation, total covered area (m^2), total count of PV modules, and solar irradiance (W/m^2), respectively.

The cost of PV is modeled by a simple linear equation:

$$C_{PV} = K_{PV}.P_{PV} \quad (6)$$

The output power of WT can be modeled as:

$$P_{WT} = \begin{cases} 0 & \text{if } v \le v_{ci} \text{ and } v \ge v_{co} \\ \frac{v^2 - v_{ci}^2}{v_r^2 - v_{ci}^2} P_{WTr} & \text{if } v_{ci} < v \le v_r \\ P_{\text{WTr}} & \text{if } v_r < v \le v_{co} \end{cases} \quad (7)$$

P_{WTr} and P_{WT} denote the rated power and output power of WT, respectively. v_r, v_{ci} and v_{co} are the rated wind speed, cut-in wind speed, and cut-on wind speed of WT, respectively.

The cost of WT is modeled by:

$$C_{WT} = K_{WT}.P_{WT} \quad (8)$$

2.5. Electric grid

Market energy costs ($/h) can be represented by a quadratic function as follows:

$$C_{Gr} = a + b.P_{Gr} + c.P_{Gr}^2 \quad (9)$$

2.6. Constraints

A. Power balance constraints

The constraint for power balance can be illustrated as:

$$\sum_{i=1}^{N_G} P_{DEG_i}^T + P_{\text{Gr}}^T = \sum_{d=1}^{N_d} P_{ld}^T \quad (10)$$

P_{ld}^T and N_d are the quantity and the total number of the loads.

B. Power generation constraints

The active power limits for each DEG in the MG are shown as:

$$P_{DEG_i\text{-}min}^T \le P_{DEG_i}^T \le P_{DEG_i\text{-}max}^T \quad (11)$$

$$P_{\text{Gr-}min}^T \le P_{\text{Gr}}^T \le P_{\text{Gr-}max}^T \quad (12)$$

Where $P_{DEG_i\text{-}min}^T$, $P^{\text{T}}{}_{Gr\text{-}min}$, $P_{DEG_i\text{-}max}^T$, and $P^{\text{T}}{}_{Gr\text{-}max}$ are the i[th] DEG and the utility active power limits at time T.

C. Spinning reserve constraints

These constraints play a crucial role in ensuring the reliability of the system amidst variations [18]:

$$P_{G_i\text{-}min}^T - P_{G_i\text{-}max}^T = \sum_{d=1}^{N_d} P_{ld}^T + R_S^T \quad (13)$$

Where R_S^T is the reserve spinning at time T.

D. Energy storage constraints

The energy storage limits can be articulated as [19]:

$$W_{\text{Bess},T} = W_{\text{Bess},T-1} + \eta_{\text{char}} P_{\text{char},T} \Delta T - \frac{1}{\eta_{\text{disch}}} P_{\text{disch},T} \Delta T \quad (14)$$

$$W_{\text{Bess,min}} \le W_{\text{Bess},T} \le W_{\text{Bess,max}} \quad (15)$$

$$P_{\text{char},T} \le P_{\text{char-max}} \text{ and } P_{\text{disch},T} \le P_{\text{disch-max}} \quad (16)$$

Where $W_{\text{Bess},T}$ and $W_{\text{Bess},T-1}$ represent the energy stored in the battery at times T and T-1, respectively. The charge and discharge rate for Δt is P_{char} and P_{disch}, while $W_{\text{Bess,min}}$, and $W_{\text{Bess,max}}$ denote the battery's energy storage limits. The η_{char} and η_{disch} indicates the battery's efficiency while charging and discharging. $P_{\text{char}-\max}$ and $P_{\text{disch}-\max}$ represent the highest rate of charge and discharge for the battery within each time interval ΔT.

E. Active power calculation for grid exchange

Active power exchange is considered a dependent variable, with grid power defined by:

$$P_{\text{Gr}}^{T} = \sum_{d=1}^{N_d} P_{ld}^{T} - \sum_{i=1}^{N_G} P_{G_i}^{T} \quad (17)$$

3. Walrus Optimizer Algorithm (WaO)

WaO is a meta-heuristic algorithm inspired by the social behavior and migration patterns of walruses. The algorithm considers the social structures and hierarchies within their communities [20]. The process of WaO optimization starts with the random generation of an initial population of candidate solutions. During the WaO iterations, these solutions move based on social and environmental signals, continually focusing on the best possible solutions.

The WaO algorithm mimics walruses' environmental responses through "safety" and "danger" signals. These signals affect the actions of every agent, thereby directing the population toward regions where optimal solutions are likely to be discovered. In this section, the key ideas behind the WaO algorithm are described.

3.1. Initialization

During the initial phase, the WaO generates a set of potential solutions (X) through a random selection method. This can be expressed mathematically as:

$$X = L_{\text{lim}} + r.\,(U_{\text{lim}} - L_{\text{lim}}) \quad (18)$$

where L_{lim} and U_{lim} denote the lower and upper limits. r is a uniform random vector that falls between 0 and 1.

The agents carrying out the optimization process are called “walrus.” Throughout the iterations, they are in a constant state of positional change.

$$X = \begin{bmatrix} X_{1,1} & X_{1,2} & \cdots & X_{1,dm} \\ X_{2,1} & X_{2,2} & \cdots & X_{2,dm} \\ \vdots & \vdots & \ddots & \vdots \\ X_{npop,1} & X_{npop,2} & \cdots & X_{npop,dm} \end{bmatrix}_{npop\times dm} \quad (19)$$

where n_{pop} and dm are the size of population and the variables dimension, respectively.

The fitness values that correspond to each search agent are kept as:

$$F_f = \begin{bmatrix} f_{\text{f1},1} & f_{\text{f1},2} & \cdots & f_{\text{f1},dm} \\ f_{\text{f2},1} & f_{\text{f2},2} & \cdots & f_{\text{f2},dm} \\ \vdots & \vdots & \ddots & \vdots \\ f_{\text{fnpop},1} & f_{\text{fnpop},2} & \cdots & f_{\text{fnpop},dm} \end{bmatrix}_{npop\times dm} \quad (20)$$

Adults make up 90% of the walrus population, while juveniles account for 10%. The proportion of adult males to females is 1:1.

3.2. Safety and danger signals

Walruses exhibit heightened vigilance concerning food-seeking and resting. In general, there are 1 to 2 walrus seeking beings that closely monitor the area. When there is a threat, these guards issue a warning and at the same time produce danger signals. The shape of the danger signal is illustrated below [21]:

$$Ds = A_{\text{s}} \,.\, \text{G} \quad (21)$$

$$\mu = 1 - t/T \quad (22)$$

$$A_{\text{s}} = 2\,.\mu \quad (23)$$

$$\text{G}_{\text{s}} = 2\,.\,r_{\text{d1}} - 1 \quad (24)$$

As the number of iterations t increases, μ decreases from 1 to 0. T represents the maximum iteration, while A_s and G_s are danger factors.

In WaO, the safety signal that corresponds to the danger signal is defined as:

$$Saf\text{-}signal = r_{\text{d2}} \quad (25)$$

where r_{d1} and r_{d2} are values chosen randomly within the range (0,1).

3.3. Migration

Walrus herds will move to areas that are more conducive to population survival when risks become too great. During this phase, the walrus's position is updated as follows [22]:

$$X_{i,k}^{t+1} = X_{i,k}^{t} + \text{mig-step} \quad (26)$$

$$\text{mig-step} = (X_s^t - X_z^t) \cdot \varphi \cdot r_{\text{d3}}^2 \quad (27)$$

$$\varphi = 1 - \frac{1}{1+\exp(-(t-(\frac{T}{2})/T\times 10)} \quad (28)$$

Where $X_{i,k}^{t}$ indicates the current position of the i$^{\text{th}}$ walrus on the k thension, and $X_{i,k}^{t+1}$ denotes its new position. The walrus movement has a step size referred to as mig-step, two vigilantes are chosen at random from the population to match positions X_s^t and X_z^t, the migration steps control factor is called φ and evolves iteratively as a smooth curve, and r_{d3} is a random value ranging from 0 to 1.

3.4. Reproduction

Walrus herds typically do not migrate; rather, they reproduce in currents when threats are at their

lowest. The positional changes of female walruses suggest that the lead walrus (X_b^t) and the male walrus ($Ma_{i,k}^t$) influence females during reproduction. Throughout the iteration, the female walrus increasingly depends on the leader and less on her mate.

$$Fem_{i,k}^{t+1} = Fem_{i,k}^t + \mu . (Ma_{i,k}^t - Fem_{i,k}^t) + (1-\mu). (X_b^t - Fem_{i,k}^t) \quad (29)$$

where $Ma_{i,k}^t$ and $Fem_{i,k}^t$ are the positions of the i^{th} male and female walruses on the k^{th} dimension. $Fem_{i,k}^{t+1}$ denotes the new position of the i^{th} female walrus along the k^{th} dimension.

Polar bears and killer whales often hunt juvenile walruses near the edge of the population. As a result, juvenile walruses must acclimatize to their new environment to evade predators.

$$Juv_{i,k}^{t+1} = (O_{sp} - Juv_{i,k}^t) \cdot J \quad (30)$$

$$O_{sp} = X_b^t + Juv_{i,k}^t \cdot LF \quad (31)$$

Where O_{sp} is the reference safety position, $Juv_{i,k}^t$ indicates the new position of the i^{th} juvenile walrus on the k^{th} dimension, and J is the juvenile walrus's distress coefficient, which is a random value between 0 and 1. Figure 1 shows the pseudo-code of WaO algorithm.

Input: Population size (n_{pop}), total number of iterations (T).
Initialize randomly the population within bounds.
Calculate the fitness value of all walruses.
while ($t \leq T$)
  Calculate Danger signal.
  if Danger signal ≥ 1
    Update the positions of each walrus (Migration phase).
  else
    Calculate Safety signal.
    if Safety signal ≥ 0.5
      Update males, females and juveniles positions separately.
    else
      if Danger signal ≥ 0.5
        Update via fleeing.
      else
        Update via gathering.
      end if
    end if
  end if
  Calculate the fitness value and update the optimal solution.
  $t = t + 1$
end while
Output Optimal solution.

Figure 1. *Pseudo-code of WaO algorithm.*

4. Results and Discussion

In this work, the tested system is based on a modified IEEE 33-bus system to evaluate the EMO using the WaO algorithm over a 24-hour period. The test system is t depicted in Figure 2. The system consists of four DERs: PV is linked via bus 13, WT linked via bus 25, MT is linked via bus 8, and DG is linked via bus 30. A BESS has been set up at Bus 18. Table 1 and table 2 provide a detailed description of the specific parameters, cost coefficients, and operational limits of the DEGs and BESS. The cost coefficient K_{PV} and K_{WT} are 0.001 \$/kWh and 0.002 \$/kWh, respectively.

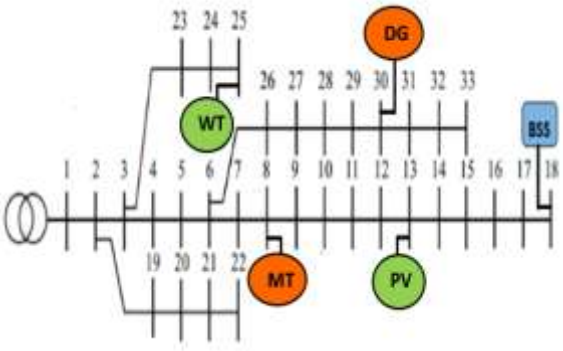

Figure 2. *One line diagram of test system*

Table 1*. Power limits of DEGs*

Units	P^{min} (MW)	P^{max} (MW)
MT	0	0.8
DG	0	0.6
PV	0	2.5
WT	0	1.5
BESS	-0.5	0.5

Table 2*. Coefficients of cost function*

Units	*a*	*b*	*c*
MT	0.004	0.18	0.5
DG	0.006	0.25	1.2
BESS	0	0.05	0

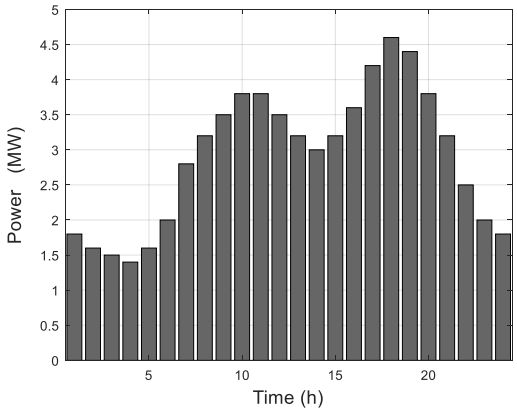

Figure 3. *Daily load demand profile*

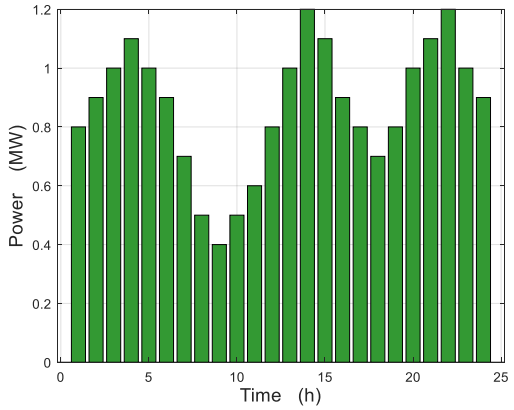

Figure 4. *Wind power availability*

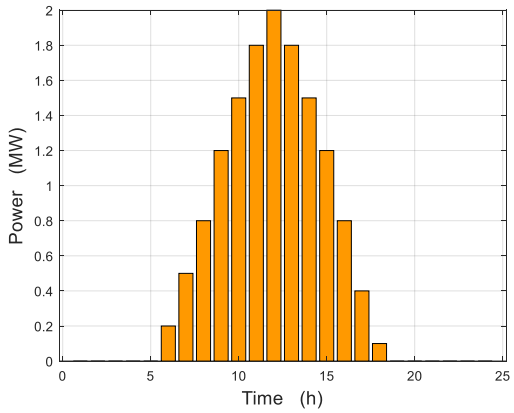

Figure 5. *PV power availability*

With a population size of 50 individuals and a maximum iteration of 200, the WaO algorithm was set up to achieve an optimal balance between exploring the search space and exploiting the best solutions. The main aim is to minimize the operational cost. To evaluate the robustness of the EMS in the face of market volatility, three case studies were designed:

Case 1: Stable and low pricing.
Case2: Moderate volatility.
Case 3: Extreme peaks and high volatility.
The daily load demand profile and renewable power availability are presented in figure 3-5.

4.1. Case 1

In this case, the market pricing is still competitive in relation to the cost of internal thermal generation. As a result, energy imports are given priority by the EMS, which minimizes the use of DG, which is more expensive to operate. The obtained results indicate that the DG operates only at certain intervals in order to flatten the profile. Figures 6–8 illustrate the MT and DG generation, PV and WT dispatch, and grid import and BESS of this case, respectively. A summary of the obtained results of this case is presented in Table 3.

Table 3. *Simulation results (Case 1)*

H (h)	P_{Grid} (MW)	P_{MT} (MW)	P_{DG} (MW)	P_{BESS} (MW)	P_{PV} (MW)	P_{WT} (MW)
1	0.86	0.35	0.03	0.36	0	0.25
2	0.41	0.32	0.05	0.02	0	0.9
3	0.58	0.27	0.03	0.18	0	0.59
4	0.09	0.17	0.02	0.12	0	1.04
5	0.45	0.05	0.1	0.08	0	0.97
6	1.62	0.05	0.01	-0.46	0.15	0.9
7	1.14	0.01	0.02	0.4	0.49	0.47
8	1.7	0.08	0.01	0.11	0.71	0.5
9	0.87	0.13	0.14	0.49	1.14	0.4
10	0.47	0.23	0.18	0.44	1.49	0.5
11	0.54	0.1	0.01	0.49	1.79	0.58
12	0.61	0.33	0.17	0	1.85	0.45
13	1.19	0.74	0.09	0.42	0.31	0.93
14	0.73	0.66	0.05	-0.36	1.11	1.16
15	0.05	0.44	0.06	0.2	1.17	1.1
16	1.07	0.55	0.17	0.15	0.41	0.89
17	2.71	0.39	0.05	0.42	0.39	0.75
18	3.23	0.32	0.08	0.49	0.09	0.7
19	2.2	0.07	0.23	0.5	0	0.77
20	2.21	0.03	0.07	0.46	0	0.99
21	1.56	0.25	0.44	-0.02	0	1.1
22	0.99	0.02	0.01	0.48	0	0.95
23	1.18	0.27	0.04	0.42	0	0.27
24	1.23	0.01	0.13	-0.05	0	0.67

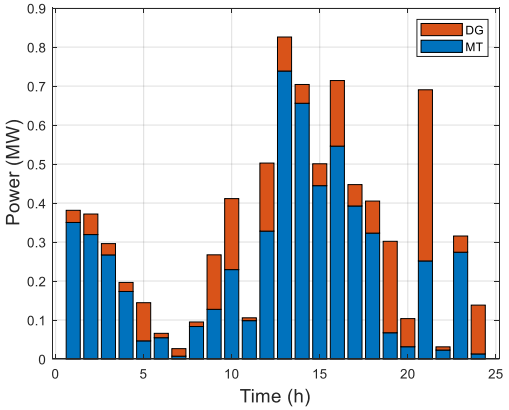

Figure 6. *MT and DG generation (Case1)*

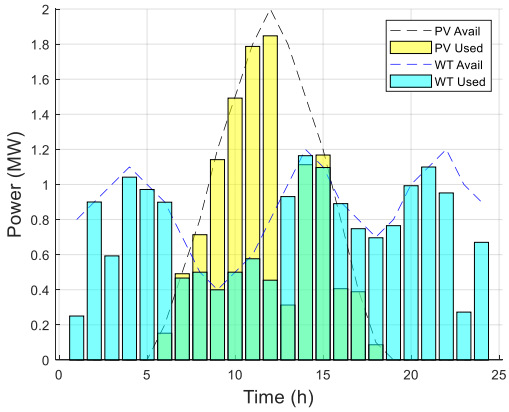

Figure 7. *PV and WT dispatch (Case 1)*

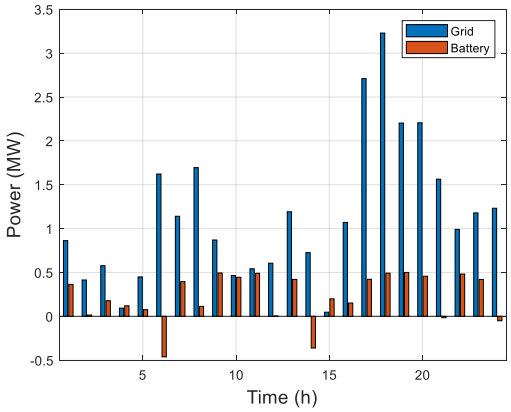

Figure 8. *Grid import and BESS (Case 1)*

4.2. Case 2

In this case, the algorithm engages in economic arbitrage as price volatility rises. The EMS increases the DEGs when grid prices beyond the cost of local generation. From the results, we can see a substantial rise in the amount of thermal generation produced locally. Figures 9–11present the MT and DG generation, PV and WT dispatch, and grid import and BESS of this case, respectively. The obtained results of this case are presented in Table 4.

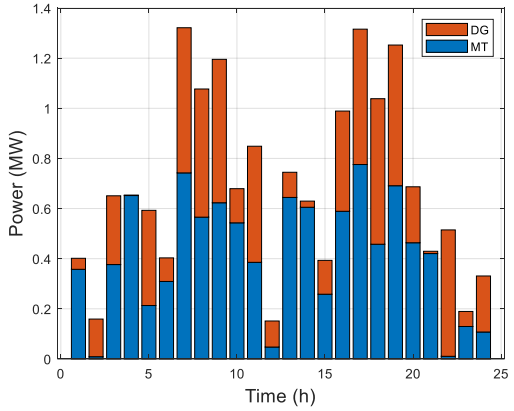

Figure 9. *MT and DG generation (Case 2)*

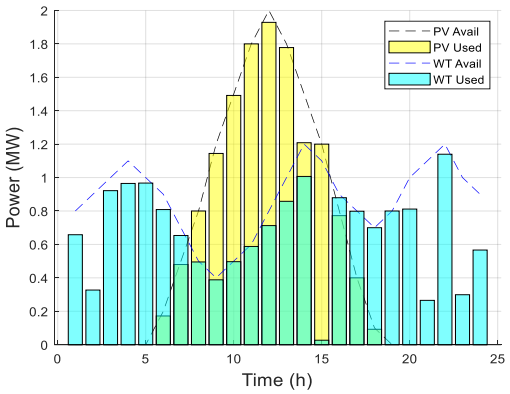

Figure 10. *PV and WT dispatch (Case 2)*

Table 4. *Simulation results (Case 2)*

H (h)	P_{Grid} (MW)	P_{MT} (MW)	P_{DG} (MW)	P_{BESS} (MW)	P_{PV} (MW)	P_{WT} (MW)
1	0.96	0.36	0.04	-0.11	0	0.66
2	1.14	0.01	0.15	0.15	0	0.33
3	0.35	0.38	0.27	-0.38	0	0.92
4	0.11	0.65	0	-0.17	0	0.96
5	0	0.21	0.38	-0.15	0	0.97
6	0.31	0.31	0.09	0.49	0.17	0.81
7	0.51	0.74	0.58	0.11	0.48	0.65
8	0.46	0.57	0.51	0.5	0.8	0.5
9	0.22	0.62	0.57	0.49	1.14	0.39
10	1.01	0.54	0.14	0.43	1.49	0.5
11	1.15	0.39	0.46	-0.12	1.8	0.59
12	0.52	0.05	0.1	0.39	1.93	0.71
13	0.05	0.64	0.1	0.04	1.78	0.86
14	0.3	0.61	0.02	-0.22	1.21	1.01
15	1.39	0.26	0.14	0.3	1.2	0.03
16	0	0.59	0.4	0.49	0.77	0.88
17	0.62	0.78	0.54	0.44	0.4	0.8
18	1.61	0.46	0.58	0.49	0.09	0.7
19	1.28	0.69	0.56	0.5	0	0.8
20	1.51	0.46	0.22	0.48	0	0.81
21	2.73	0.42	0.01	-0.15	0	0.27
22	1.04	0.01	0.5	-0.04	0	1.14
23	2.07	0.13	0.06	-0.35	0	0.3
24	0.64	0.11	0.22	0.36	0	0.57

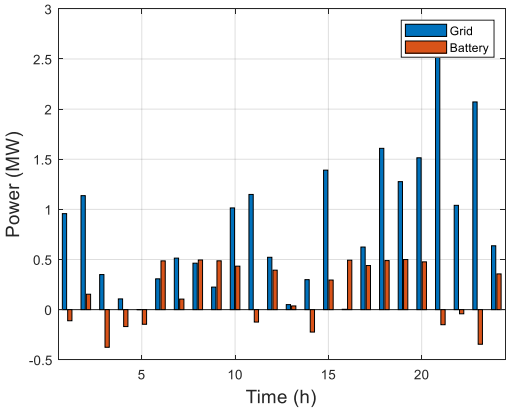

Figure 11. *Grid import and BESS (Case 2)*

4.3. Case 3

This case represents a critical stress test with prices peaking. The EMS strategy shifts drastically to minimize grid dependency during peak hours (Hours 16-19). The DEGs use their maximum power during times of medium and high lead levels when the market price is brought to its true worth. Additionally, the MG exports excess energy to the utility for the majority of the day. Figures 12–14 show the MT and DG generation, PV and WT dispatch, and grid import and BESS of this case, respectively. The obtained results of this case are presented in Table 5. Figure 15 and figure 16 present the convergence of the total cost and the energy market price of the three

Table 5. *Simulation results (Case 3)*

H (h)	P_{Grid} (MW)	P_{MT} (MW)	P_{DG} (MW)	P_{BESS} (MW)	P_{PV} (MW)	P_{WT} (MW)
1	0.42	0.03	0.5	0.36	0	0.73
2	1.41	0.57	0.2	-0.44	0	0.09
3	0.48	0.66	0.26	0.09	0	0.15
4	0.54	0.05	0.12	0.17	0	0.48
5	0.01	0.27	0.49	-0.04	0	0.91
6	0.05	0.09	0.46	0.41	0.17	0.8
7	0.11	0.58	0.56	0.48	0.47	0.69
8	0.11	0.66	0.52	0.21	0.76	0.49
9	0.25	0.36	0.54	0.5	1.16	0.38
10	1.2	0.2	0.46	0.49	1.5	0.5
11	1.65	0.25	0.29	0.43	1.13	0.25
12	0.24	0.62	0.58	-0.47	1.91	0.8
13	1.96	0.17	0.11	0.01	0.96	0.46
14	0.01	0.65	0.09	0.48	1.26	0.12
15	0.27	0.34	0.39	0.36	0.98	1.06
16	0.56	0.8	0.56	0.01	0.77	0.9
17	1.29	0.8	0.55	0.49	0.35	0.8
18	1.37	0.67	0.59	0.49	0.1	0.7
19	2.01	0.25	0.31	0.49	0	0.68
20	1.43	0.58	0.5	0.02	0	0.94
21	1.02	0.68	0.54	-0.09	0	1.09
22	0.61	0.61	0.04	0.43	0	1.16
23	0.91	0.03	0.08	-0.12	0	0.95
24	1.32	0.03	0.13	0.49	0	0.01

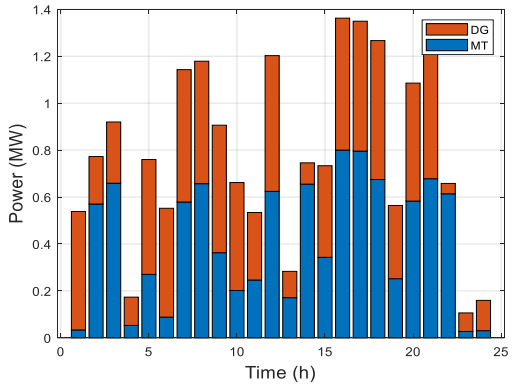

Figure 12. *MT and DG generation (Case 3)*

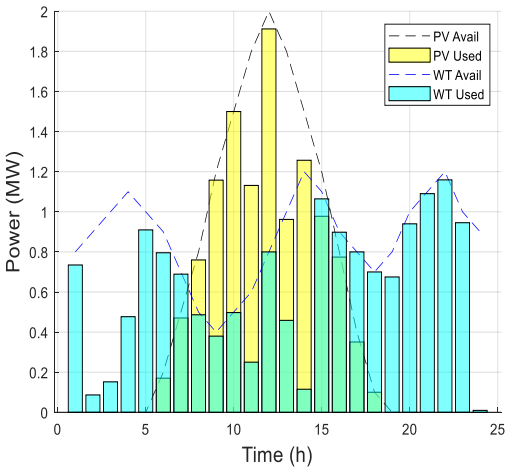

Figure 13. *PV and WT dispatch (Case 3)*

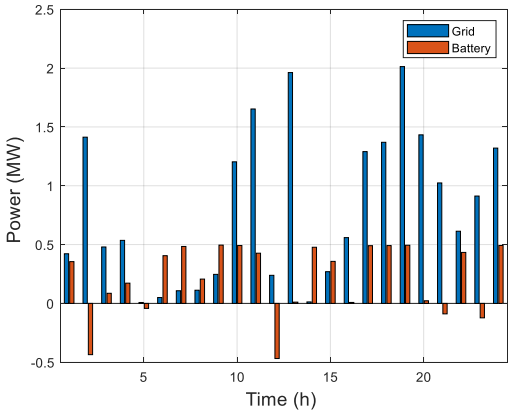

Figure 14. *Grid import and BESS (Case 3)*

case studies, respectively. WaO algorithm demonstrate consistent convergence properties in every case. According to the computational results, taking renewable sources into account as dispatchable enables accurate power balance and lessens the need for costly penalty infractions.

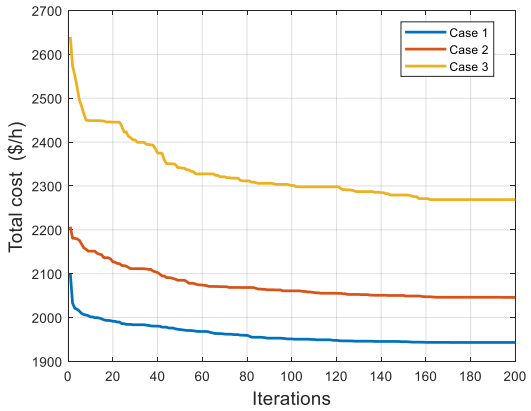

Figure 15. *Convergence of the total cost.*

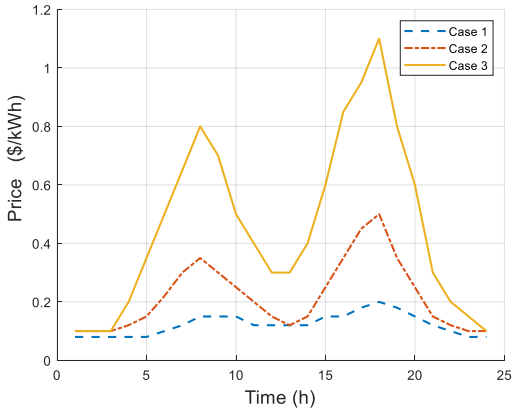

Figure 16. *Energy market price.*

5. Conclusion

This paper presents an OEM based on the WaO algorithm for MG that is linked to numerous DEGs and a BESS. The study showed that the proposed algorithm effectively reduces operational costs and

achieves significant savings by optimizing the scheduling of DEGs and storage through simulations of the IEEE 33-bus system under three different pricing scenarios. In volatile markets, the system demonstrates robust resilience by optimizing the use of DEGs and BESS to minimize operational expenses and lessen the effects of elevated electricity costs. The proposed method guarantees technical reliability and ensures that the supply-demand balance is maintained at all times.

Author Statements:

- **Ethical approval:** The conducted research is not related to either human or animal use.
- **Conflict of interest:** The authors declare that they have no known competing financial interests or personal relationships that could have appeared to influence the work reported in this paper
- **Acknowledgement:** The authors declare that they have nobody or no-company to acknowledge.
- **Author contributions:** The authors declare that they have equal right on this paper.
- **Funding information:** The authors declare that there is no funding to be acknowledged.
- **Data availability statement:** The data that support the findings of this study are available on request from the corresponding author. The data are not publicly available due to privacy or ethical restrictions.

Reference

[1] J. Jiang, M. Xue, and G. Geng, "Energy management of microgrid in grid-connected and stand-alone modes," IEEE Trans. Power Syst., vol. 28, no. 3, pp. 3380–3389, Aug. 2013.

[2] A. Amir, H. Shareef, and F. Awwad, "Energy management in a standalone microgrid: A split-horizon dual-stage dispatch strategy," Energies, vol. 16, no. 8, p. 3400, Apr. 2023.

[3] N. Z. Xu and C. Y. Chung, "Algorithms for multi-agent based distribution networks: A survey," Renewable Energy, vol. 131, pp. 244–258, Feb. 2019.

[4] S. Mirjalili, S. M. Mirjalili, and A. Lewis, "Grey wolf optimizer," Adv. Eng. Softw., vol. 69, pp. 46–61, Mar. 2014.

[5] J. Kennedy and R. Eberhart, "Particle swarm optimization," Proc. IEEE Int. Conf. Neural Netw., vol. 4, pp. 1942–1948, Dec. 1995.

[6] A. Arabali, M. Ghofrani, M. Etezadi-Amoli, M. S. Fadali, and Y. Baghzouz, "Genetic-algorithm-based optimization approach for energy management," *IEEE Transactions on Power Delivery*, vol. 28, no. 1, pp. 162–170, Jan. 2013.

[7] P. Li, W. Xu, Z. Zhou, and R. Li, "Optimized operation of microgrid based on gravitational search algorithm," in *2013 International Conference on Electrical Machines and Systems (ICEMS)*, pp. 338–342, Oct. 2013.

[8] S. Mandal and K. K. Mandal, "Optimal energy management of microgrids under environmental constraints using chaos enhanced differential evolution," *Renewable Energy Focus*, vol. 34, pp. 129–141, Sep. 2020.

[9] Y. M. Alsmadi *et al.*, "Optimal configuration and energy management scheme of an isolated micro-grid using Cuckoo search optimization algorithm," *Journal of the Franklin Institute*, vol. 356, no. 8, pp. 4191–4214, May 2019.

[10] A. P. Lopes, C. L. Moreira, and A. G. Madureira, "Defining control strategies for microgrids islanded operation," *IEEE Transactions on Power Systems*, vol. 21, no. 2, pp. 916–924, May 2006.

[11] Y. Li, S. Q. Mohammed, G. S. Nariman, N. Aljojo, A. Rezvani, and S. Dadfar, "Energy management of microgrid considering renewable energy sources and electric vehicles using the backtracking search optimization algorithm," *Journal of Energy Resources Technology*, vol. 142, no. 5, May 2020.

[12] B. Hernández-Ocaña, J. Hernández-Torruco, O. Chávez-Bosquez, M. B. Calva-Yáñez, and E. A. Portilla-Flores, "Bacterial foraging-based algorithm for optimizing the power generation of an isolated microgrid," *Applied Sciences*, vol. 9, no. 6, p. 1261, Mar. 2019.

[13] M. A. Kamarposhti, I. Colak, and K. Eguchi, "Optimal energy management of distributed generation in micro-grids using artificial bee colony algorithm," *Mathematical Biosciences and Engineering*, vol. 18, no. 6, pp. 7402–7418, 2021.

[14] K. S. Nimma, M. D. A. Al-Falahi, H. D. Nguyen, S. D. G. Jayasinghe, T. S. Mahmoud, and M. Negnevitsky, "Grey wolf optimization-based optimum energy-management and battery-sizing method for grid-connected microgrids," *Energies*, vol. 11, no. 4, p. 847, Apr. 2018.

[15] B. Bentouati, A. Khelifi, A. M. Shaheen, and R. A. El-Sehiemy, "An enhanced moth-swarm algorithm for efficient energy management based multi dimensions OPF problem," *Journal of Ambient Intelligence and Humanized Computing*, vol. 12, no. 10, pp. 9499–9519, Oct. 2021.

[16] Xuejie Wang, Yanchao Ji, Jianze Wang, Yuanjun Wang and Lei Qi, "Optimal energy management of microgrid based on multi-parameter dynamic programming", International Journal of Distributed Sensor Networks, Vol. 16(6), 2020.

[17] Aslam Amir, Hussain Shareef and Falah Awwad, "Energy Management in a Standalone Microgrid: A Split-Horizon Dual-Stage Dispatch Strategy", Energies, 16, 3400, 2023.

[18] Wu H., Liu X., Ding M. "Dynamic economic dispatch of a microgrid: Mathematical Models and Solution Algorithm", International Journal of Electrical Power and Energy Systems, vol. 63, pp. 336–346, 2014.

[19] A. A. Moghaddam, A. Seifi, T. Niknam, and M. R. A. Pahlavani, "Multi-objective operation management of a renewable MG (micro-grid) with back-up micro-

turbine/fuel cell/battery hybrid power source", Energy, vol. 36, pp. 6490–6507, 2011.

[20] Ark Dev, Kunalkumar Bhatt, Bappa Mondal and Vineet Kumar, "Enhancing load frequency control and automatic voltage regulation in Interconnected power systems using the Walrus optimization algorithm", Scientific Reports 2024.

[21] Mokhtar Said, Essam H. Houssein, Eman Abdullah Aldakheel, Doaa Sami Khafaga, and Alaa A. K. Ismaeel, "Performance of the Walrus Optimizer for solving an economic load dispatch problem", AIMS Mathematics, 9(4): 10095–10120, 2024.

[22] Mohamed A. M. Shaheen, Hany M. Hasanien, S. F. Mekhamer and Hossam E. A. Talaat, "Walrus optimizer-based optimal fractional order PID control for performance enhancement of offshore wind farms ", Scientific Reports 14:17636, 2024.